

### SPACECRAFT AND INSTRUMENT DESCRIPTION

This image mosaic is based on observations acquired by the Mercury Dual Imaging System (MDIS; Hawkins and others, 2009), an instrument on the National Aeronautics and Space Agency (NASA) Mercury Surface, Space Environment, Geochemistry, and Ranging (MESSENGER) spacecraft (Solomon and others, 2007). MDIS consists of two cameras, a wide angle camera (WAC) and a narrow angle camera (NAC). The WAC is a 4-element refractive telescope having a focal length of 78 mm and a collecting area of 48 mm<sup>2</sup>. A 12-position filter wheel provides color imaging over the spectral range of the charge-coupled device (CCD) detector. Eleven spectral filters spanning the range from 395 nanometers (nm) to 1,040 nm are defined to cover wavelengths diagnostic of different surface materials. The twelfth position is a broad-band filter for optical navigation. The filters are arranged on the filter wheel in such a way as to provide complementary passbands (for example, 3- and 4-color imaging) in adjacent positions (Denevi and others, 2016). The NAC is an off-axis reflective telescope with a 550-mm focal length and a collecting area of 462 mm<sup>2</sup>. The NAC has an identical CCD detector with a single medium-band filter (100 nm wide), centered at 750 nm to match to the corresponding WAC filter 7 (or G filter for monochrome imaging (Hash and others, 2015)).

### MAP DESCRIPTION

This global mosaic includes the Basemap Data Records (BDR) compiled using NAC and WAC 750-nm images that best fit the intended illumination geometry of low emission angle and incidence angle near 74°. Prior to mosaicking, the images were photometrically normalized to a solar incidence angle ( $i$ ) = 30°, emission angle ( $e$ ) = 0°, and phase angle ( $\alpha$ ) = 30° at a spatial sampling of 256 pixels per degree (~166 meter per pixel at the equator). The 30° incidence angle was found to minimize shadows while including topographic shading. This edition, version 2, was released on May 12, 2017, as 15 tiles to the Planetary Data System (PDS) MESSENGER archive (Hash, 2013).

### PROJECTION

The Mercator projection is used between latitudes ±57°, with a central meridian at 0° longitude and latitude equal to the nominal scale at 0°. The polar stereographic projection is used for the regions north of the +55° parallel and south of the -55° parallel, with a central meridian set for both at 0° and a latitude of true scale at +90° and -90°, respectively. The adopted spherical radius used to define the map scale is 2439.4 km (Perry and others, 2015).

### COORDINATE SYSTEM

The orientation model for Mercury has been updated using improved pole position and short-period longitude libration information from Margot (2009). The International Astronomical Union (IAU) Working Group, since its original report (Davies and others, 1980), recommends the use of the crater Hun Kal (which means "twenty" in the Mayan language) to define the 20° west longitude meridian. Therefore, the value of the prime meridian (W0) used previously (W0 = 329.548°; Robinson and others, 1999) but corrected for libration terms at J2000.0 results in a new recommended value of W0 = 329.5988° (Stark, 2016). The pole position is given by an updated model by Stark, with the J2000.0 right ascension of the pole as 281.0103-0.03287 and the declination as 61.4155-0.0049T, where T is the number of Julian centuries from J2000.0 (Stark, 2017).

Using this prime meridian, the mosaic was constructed from overlapping NAC and WAC 750-nm images and controlled using NASA's updated Navigation and Ancillary Information Facility (NAIF) SPICE (Spacecraft, Planet, Instrument, C-matrix, Events, Acton, 1996) kernels (known as c-smithed kernels) and a global digital elevation model (DEM), both derived using a least-squares bundle adjustment of common features. Images were orthorectified using this derived DEM. Empirically, misregistration errors between images decreased generally to the pixel scale of the map (~0.2 km) in most locations. Derivation of c-smithed kernels and the DEM for end-of-mission data products was described by Becker and others (2016).

Longitudes are shown in both positive West (shown in black) and East (shown in red). Positive West is the default longitude system recommended by the IAU (Archinal and others, 2011), but positive East has been used for all MESSENGER map products.

### MAPPING TECHNIQUES

Included in this global mosaic are BDRs created with images from any campaign that best fit the intended illumination geometry. A campaign refers to a planned period of image acquisition during a mission. To prepare the images for publication, the original PDS tiles were map projected into Mercator and Polar Stereographic projections with a resolution of ~166 meter per pixel. The original reflectance values (1/F) were stretched from a minimum of 0.000867 to a maximum of 0.220197 to 8 bits (0 to 255) using a linear stretch. Finally, the images were then scaled to 1:20,000,000 for the Mercator part and 1:12,157,366 for the two polar stereographic parts with a resolution of 300 pixels per inch. The two projections have a common scale at ±56° latitude.

### NOMENCLATURE

Feature names on this sheet have been approved by the IAU. All features greater than 100 km in diameter or length were included unless they were not visible at the printed map scale. Some selected well-known features less than 100 km in diameter or length were also included. For a complete list of the IAU-approved nomenclature for Mercury, see the Gazetteer of Planetary Nomenclature at <https://planetarynames.wr.usgs.gov>.

### ACKNOWLEDGMENTS

The collection of the data used in the production of this map was made possible by NASA and the MESSENGER team. The production of the map itself and publication costs were funded by a NASA and USGS Interagency Agreement.

### REFERENCES CITED

- Acton, C.H., 1996, Ancillary Data Services of NASA's Navigation and Ancillary Information Facility: Planetary and Space Science, v. 44, no. 1, p. 65–70, <https://naif.jpl.nasa.gov/naif/>.
- Archinal, B.A. (chair), A'Hearn, M.F., Bowell, E., Conrad, A., Consolmagno, G.J., Courtin, R., Fukushima, T., Hestroffer, D., Hilton, J.L., Krasinsky, G.A., Neumann, G., Oberst, J., Seidelmann, P.K., Stooke, P., Tholen, D.J., Thomas, P.C., and Williams, I.P., 2011, Report of the IAU Working Group on Cartographic Coordinates and Rotational Elements—2009: Celestial Mechanics and Dynamical Astronomy, v. 109, no. 2, p. 101–135, <https://doi.org/10.1007/s10569-010-9320-4>.
- Becker, K.J., Robinson, M.S., Becker, T.L., Weller, L.A., Edmondson, L., Neumann, G.A., Perry, M.E., and Solomon, S.C., 2016, First global digital elevation model of Mercury: Lunar and Planetary Science XLVII abstract 2959.
- Davies, M.E., Abalakin, V.K., Cross, C.A., Duncombe, R.L., Masursky, H., Morando, B., Owen, T.C., Seidelmann, P.K., Sinclair, A.T., Wilkins, G.A., and Tjufin, Y.S., 1980, Report of the IAU Working Group on Cartographic Coordinates and Rotational Elements of the Planets and Satellites: Celestial Mechanics and Dynamical Astronomy, v. 22, p. 205–230.
- Denevi, B.W., Seelos, F.P., Ernst, C.M., Keller, M.R., Chabot, N.L., Murchie, S.L., Domingue, D.L., Hash, C.D., and Blewett, D.T., 2016, Final calibration and multispectral map products from the Mercury Dual Imaging System wide-angle camera on MESSENGER: Lunar and Planetary Science XLVII abstract 1264, <https://www.hou.usra.edu/meetings/lpsc2016/pdf/1264.pdf>.
- Hash, C., 2013, MESSENGER MDIS Map Projected Basemap RDR V1.0: NASA Planetary Data System, <https://pds-imaging.jpl.nasa.gov/volumes/mess.html>.
- Hash, C., Esprituro, R., Malaret, E., Prockter, L., Murchie, S., Mick, A., and Ward, J., 2015, MESSENGER Mercury Dual Imaging System (MDIS) Experiment Data Record (EDR) Software Interface Specification (SIS): The Johns Hopkins University, Applied Physics Laboratory, MDIS EDR SIS version 2.21, [https://ndimga2.wr.usgs.gov/archives/mess-e-v-b-mdis-2-edr-ravdata-v1.0/MSGRMDS\\_1001/DOCUMENT/MDISEDRSIS.PDF](https://ndimga2.wr.usgs.gov/archives/mess-e-v-b-mdis-2-edr-ravdata-v1.0/MSGRMDS_1001/DOCUMENT/MDISEDRSIS.PDF).
- Hawkins, S.E., III, Murchie, S.L., Becker, K.J., Selby, C.M., Turner, F.S., Nobel, M.W., Chabot, N.L., Choo, T.H., Darlington, E.H., Denevi, B.W., Domingue, D.L., Ernst, C.M., Holsclaw, G.M., Laso, N.R., McClintock, W.E., Prockter, L.M., Robinson, M.S., Solomon, S.C., and Stemer, R.E., II, 2009, In-flight performance of MESSENGER's Mercury Dual Imaging System, in Hoover, B., Levin, G.V., Rozanov, A.Y., and Retherford, K.D., eds., Instruments and Methods for Astrobiology and Planetary Missions XII: Bellingham, Wash., SPIE, Paper 74410Z, 12 p.
- Margot, J.L., 2009, A Mercury orientation model including non-zero obliquity and librations: Celestial Mechanics and Dynamical Astronomy, v. 105, p. 329–336, <https://doi.org/10.1007/s10569-009-9234-1>.
- Perry, M.E., Neumann, G.A., Phillips, R.J., Barnouin, O.S., Ernst, C.M., Kahan, D.S., Solomon, S.C., Zuber, M.T., Smith, D.R., Hauck, S.A., II, Peale, S.J., Margot, J.L., Mazario, E., Johnson, C.L., Gaskell, R.W., Roberts, J.H., McNutt, R.L., Jr., and Oberst, J., 2015, The low-degree shape of Mercury: Geophysical Research Letters, v. 42, p. 6951–6958, <https://doi.org/10.1002/2015GL065101>.
- Robinson, M.S., Davies, M.E., Colvin, T.R., and Edwards, K., 1999, A revised control network for Mercury: Journal of Geophysical Research, v. 104, p. 30847–30852.
- Solomon, S.C., McNutt, R.L., Gold, R.E., and Domingue, D.L., 2007, MESSENGER mission overview: Space Science Reviews, v. 131, p. 3–39, <https://doi.org/10.1007/s11214-007-9247-6>.
- Stark, A., 2015, The prime meridian of the planet Mercury: DLR and Technische Universität Berlin, [http://naif.jpl.nasa.gov/pub/naif/pds/data/mess-e-v-b-spice-6-v1.0/messp\\_1000/document/messp\\_prime\\_meridian.pdf](http://naif.jpl.nasa.gov/pub/naif/pds/data/mess-e-v-b-spice-6-v1.0/messp_1000/document/messp_prime_meridian.pdf).
- Stark, A., Oberst, J., Preusker, F., Burmeister, S., Steinbrügge, H., 2017, The reference frames of Mercury after MESSENGER, arXiv preprint arXiv:1710.09686.

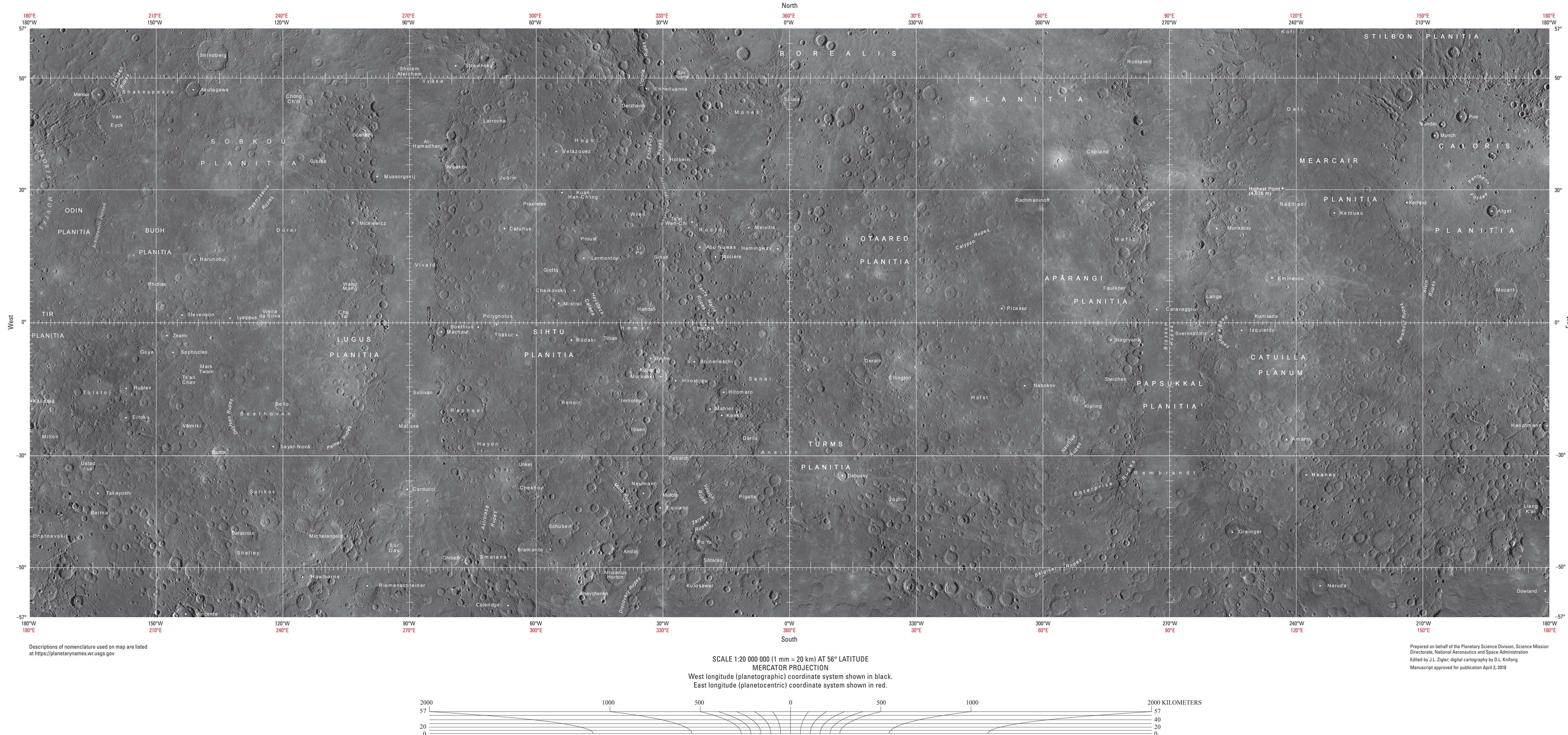
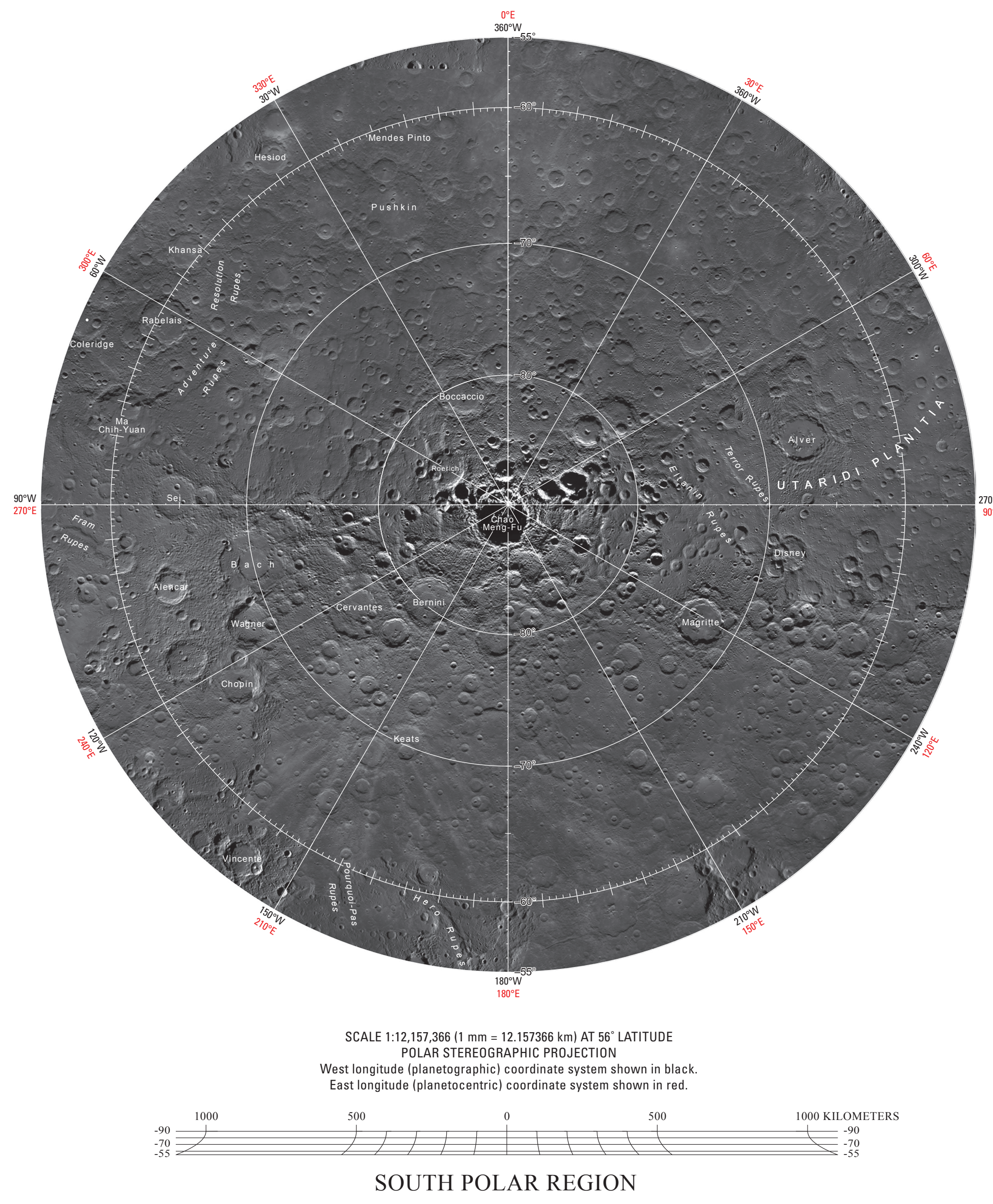


## Image Map of Mercury

By

Marc A. Hunter,<sup>1</sup> Trent M. Hare,<sup>1</sup> Rosalyn K. Hayward,<sup>1</sup> Nancy L. Chabot,<sup>2</sup> Christopher D. Hash,<sup>3</sup>  
Brett W. Denevi,<sup>2</sup> Carolyn M. Ernst,<sup>2</sup> Scott L. Murchie,<sup>2</sup> David T. Blewett,<sup>2</sup> Erick R. Malaret,<sup>2</sup> and Sean C. Solomon<sup>4</sup>  
2018

<sup>1</sup>U.S. Geological Survey,  
<sup>2</sup>Johns Hopkins University,  
<sup>3</sup>Applied Coherent Technology Corp.,  
<sup>4</sup>Columbia University